

Manifestations of High Density QCD in the first RHIC data

Dmitri Kharzeev^{a)} and Eugene Levin^{b)}a) Physics Department,
Brookhaven National Laboratory,
Upton, NY 11973 - 5000, USAb) HEP Department, School of Physics,
Raymond and Beverly Sackler Faculty of Exact Science,
Tel Aviv University, Tel Aviv 69978, Israel

Abstract

We derive a simple analytical scaling function which embodies the predictions of high density QCD on the energy, centrality, rapidity, and atomic number dependences of hadron multiplicities in nuclear collisions. Both centrality and rapidity dependences of hadron multiplicity in Au-Au collisions as measured at RHIC at $\sqrt{s} = 130$ GeV are well described in this approach. The centrality and rapidity dependences of hadron multiplicity at $\sqrt{s} = 200$ GeV run at RHIC are predicted; the variation of these dependences with energy appear different from other approaches, and can be used as an important test of the ideas based on parton saturation and classical Chromo-Dynamics.

Relativistic heavy ion collisions allow to probe QCD in the non-linear regime of high parton density and high color field strength. It has been conjectured long time ago that the dynamics of QCD in the high density domain may become qualitatively different: in parton language, this is best described in terms of parton saturation [1, 2, 3], and in the language of color fields { in terms of the classical Chromo-Dynamics [4, 5, 6, 7]. In this high density regime, the transition amplitudes are dominated not by quantum fluctuations, but by the configurations of classical field containing large, $l = s$, numbers of gluons. One thus uncovers new non-linear features of QCD, which cannot be investigated in the more traditional applications based on the perturbative approach. The classical color fields in the initial nuclei (the "color glass condensate" [4, 5]) can be thought of as either perturbatively generated, or as being a topologically non-trivial superposition of the Weizsacker-Williams radiation and the quasi-classical vacuum fields [8, 9].

Recently, with the advent of RHIC, the heavy ion program has entered the era of collider experiments. First RHIC results on hadron multiplicities have been presented [10, 11, 12, 13].

The established experimental centrality dependence is so far in accord with predictions [7] based on high density QCD. (For alternative approaches, see [14, 15, 16, 17]). Rapidity dependence of the hadron multiplicity has recently been presented as well, and it is important to check if it agrees with the high density QCD calculations as well. It is also most timely to make predictions for the higher energy, $\sqrt{s} = 200$ GeV run. These are the objectives of this paper.

Let us begin by presenting a brief and elementary introduction into the concept of parton saturation [1]. Consider an external probe J interacting with the nuclear target of atomic number A . At small values of Bjorken x , by uncertainty principle the interaction develops over large longitudinal distances $z \sim 1/(m x)$, where m is the nucleon mass. As soon as z becomes larger than the nuclear diameter, the probe cannot distinguish between the nucleons located on the front and back edges of the nucleus, and all partons within the transverse area $\sim 1/Q^2$ determined by the momentum transfer Q participate in the interaction coherently. The density of partons in the transverse plane is given by

$$\rho_A \sim \frac{xG_A(x;Q^2)}{R_A^2} \sim A^{1/3}; \quad (1)$$

where we have assumed that the nuclear gluon distribution scales with the number of nucleons A . The probe interacts with partons with cross section $\sigma_s \sim Q^{-2}$; therefore, depending on the magnitude of momentum transfer Q , atomic number A , and the value of Bjorken x , one may encounter two regimes:

$\rho_A \ll 1$ { this is a familiar "dilute" regime of incoherent interactions, which is well described by the methods of perturbative QCD;

$\rho_A \gg 1$ { in this regime, we deal with a dense parton system. Not only do the "leading twist" expressions become inadequate, but also the expansion in higher twists, i.e. in multi-parton correlations, breaks down here.

The border between the two regimes can be found from the condition $\rho_A \sim 1$; it determines the critical value of the momentum transfer ("saturation scale" [1, 4]) at which the parton system becomes too dense to the probe¹:

$$Q_s^2 \sim \frac{xG_A(x;Q_s^2)}{R_A^2}; \quad (2)$$

In this regime, the number of gluons from (2) is given by

$$xG_A(x;Q_s^2) \sim \frac{1}{\sigma_s(Q_s^2)} Q_s^2 R_A^2; \quad (3)$$

where $Q_s^2 R_A^2 \sim A$. One can see that the number of gluons is proportional to the inverse of $\sigma_s(Q_s^2)$, and becomes large in the weak coupling regime. In this regime, as we shall now discuss, the dynamics is likely to become essentially classical.

¹Note that since $Q_s^2 \sim A^{1/3}$, this expression in the target rest frame can also be understood as describing a broadening of the transverse momentum resulting from the multiple re-scattering of the probe.

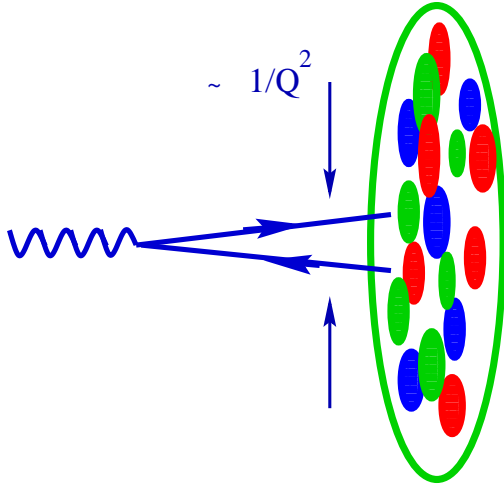


Figure 1: Hard probe interacting with the nuclear target resolves the transverse area $\sim 1/Q^2$ (Q^2 is the square of the momentum transfer) and, in the target rest frame, the longitudinal distance $\sim 1/(m \times)$ (m is the nucleon mass and x { Bjorken variable).

The condition (2) can be rederived in a way [18] which illustrates the link between the saturation and classical Yang-Mills fields [4]. As a first step, let us re-scale the gluon fields in the Lagrangian

$$L = \frac{1}{4} G^a G^a + \sum_f q_f^a (i \not{D} - m_f) q_f^a; \quad (4)$$

as follows: $A^a \rightarrow \tilde{A}^a = g A^a$. In terms of new fields, $\tilde{G}^a = g G^a = \partial A^a - \partial A^a + f^{abc} A^b A^c$, and the dependence of the action corresponding to the Lagrangian (4) on the coupling constant is given by

$$S = \int \frac{1}{g^2} \tilde{G}^a \tilde{G}^a d^4x; \quad (5)$$

Let us now consider a classical configuration of gluon fields; by definition, \tilde{G}^a in such a configuration does not depend on the coupling, and the action is large, $S \gg \hbar$. The number of quanta in such a configuration is then

$$N_g = \frac{S}{\hbar} = \frac{1}{s} \int V_4; \quad (6)$$

where we rewrote (5) as a product of four-dimensional action density \mathcal{L}_4 and the four-dimensional volume V_4 .

The effects of non-linear interactions among the gluons become important when $\partial A \sim A^2$ (this condition can be made explicitly gauge invariant if we derive it from the expansion of a correlation function of gauge-invariant gluon operators, e.g., \tilde{G}^2). In momentum space, this equality corresponds to

$$Q_s^2 \sim A^2 \sim (\tilde{G}^2)^{1/2} = \frac{P}{4}; \quad (7)$$

Q_s is the typical value of the gluon momentum below which the interactions become essentially non-linear.

Consider now a nucleus A boosted to a high momentum. By uncertainty principle, the gluons with transverse momentum Q_s are extended in the longitudinal and proper time directions by

Q_s ; since the transverse area is R_A^2 , the four-volume is $V_4 = R_A^2 Q_s^2$. The resulting four-density from (6) is then

$$N_g = \frac{N_g}{V_4} = \frac{N_g Q_s^2}{R_A^2} Q_s^4; \quad (8)$$

where at the last stage we have used the non-linearity condition (7), $N_g = Q_s^4$. It is easy to see that (8) coincides with the saturation condition (2), since the number of gluons in the infinite momentum frame $N_g = xG(x; Q_s^2)$. This simple derivation illustrates that the physics in the high-density regime can potentially be understood in terms of classical gluon fields. This correspondence allowed to formulate an effective quasi-classical theory [4], which is a subject of vigorous investigations at present (see, e.g., [5, 6]).

In nuclear collisions, the saturation scale becomes a function of centrality; a generic feature of the quasi-classical approach – the proportionality of the number of gluons to the inverse of the coupling constant (6) – thus leads to definite predictions [7] on the centrality dependence of multiplicity:

$$\frac{dN}{d} = c N_{part} xG(x; Q_s^2); \quad (9)$$

where $xG(x; Q_s^2) = \ln(Q_s^2 = \frac{2}{Q_{CD}})$, N_{part} is the number of participants, and c is the "parton liberation" coefficient, which was determined [7] from the experimental multiplicity to be

$$c = 1.23 \pm 0.20; \quad (10)$$

This value is on the order of unity [19], and agrees with the lattice [20] and analytical [21] calculations. The prediction (9) so far is in accord with the data coming from RHIC [10, 11, 12, 13]. Let us now make predictions for $\sqrt{s} = 200$ GeV collisions based on this picture.

The energy dependence of the hadron production is determined by the variation of saturation scale Q_s with Bjorken $x = Q_s^2 / \sqrt{s}$. This variation, in turn, is determined by the x dependence of the gluon structure function. In the saturation approach, the gluon distribution is related to the saturation scale by Eq.(2). A good description of HERA data is obtained with saturation scale $Q_s^2 = 1.2$ GeV² with W -dependence ($W = \sqrt{s}$ is the center-of-mass energy available in the photon(nucleon system) [22])

$$Q_s^2 = W^{-\lambda}; \quad (11)$$

where $\lambda = 0.25 \pm 0.3$. In spite of significant uncertainties in the determination of the gluon structure functions, perhaps even more important is the observation [22] that the HERA data exhibit scaling when plotted as a function of variable

$$x = \frac{Q^2}{Q_0^2} \frac{x}{x_0}; \quad (12)$$

where the value of x_0 is again within the limits $\lambda = 0.25 \pm 0.3$. In high density QCD, this scaling is a consequence of the existence of dimensionful scale [1, 4])

$$Q_s^2(x) = Q_0^2(x_0 = x); \quad (13)$$

The formula (9) can be equivalently rewritten as (see [7] for details)

$$\frac{dN}{d} = S_A \frac{Q_s^2}{s(Q_s^2)}; \quad (14)$$

where S_A is the nuclear overlap area, determined by atomic number and the centrality of collision.

The energy dependence of multiplicity is thus (up to a logarithmic correction, which is small for the energy interpolation that we make) given by

$$\frac{dN}{d}(\sqrt{s} = 200 \text{ GeV}) \approx \frac{200}{130} \frac{dN}{d}(\sqrt{s} = 130 \text{ GeV}) = (1.10 \pm 1.14) \frac{dN}{d}(\sqrt{s} = 130 \text{ GeV}); \quad (15)$$

indicating that the hadron multiplicity is expected to raise in the $\sqrt{s} = 200 \text{ GeV}$ run by about $10 \pm 14\%$. Taking the PHOBOS number for charged multiplicity at $\sqrt{s} = 130 \text{ GeV}$ for the 6% centrality cut, $dN/d = 555 \pm 12(\text{stat}) \pm 35(\text{syst})$ [25], one gets a prediction of

$$dN/d = 616 \pm 634 \quad (16)$$

for the $\sqrt{s} = 200 \text{ GeV}$ (these are the central values not taking into account the error bars of the $\sqrt{s} = 130 \text{ GeV}$ measurement).

One can also try to extract the value of α_s from the energy dependence of hadron multiplicity measured by PHOBOS at $\sqrt{s} = 130 \text{ GeV}$ and at $\sqrt{s} = 56 \text{ GeV}$; this procedure yields $\alpha_s \approx 0.37$, which is larger than the value inferred from the HERA data (and is very close to the value $\alpha_s \approx 0.38$, resulting from the naive saturation calculations [15]).

Let us now proceed to the calculation of the (pseudo)rapidity and centrality dependences. We need to evaluate the leading tree diagram describing emission of gluons on the classical level, see Fig. 2. Let us introduce the unintegrated gluon distribution $\mathcal{G}_A(\mathbf{x}; k_t^2)$ which describes the probability to find a gluon with a given \mathbf{x} and transverse momentum k_t inside the nucleus A . As follows from this definition, the unintegrated distribution is related to the gluon structure function by

$$xG_A(\mathbf{x}; p_t^2) = \int^{p_t^2} dk_t^2 \mathcal{G}_A(\mathbf{x}; k_t^2); \quad (17)$$

when $p_t^2 > Q_s^2$, the unintegrated distribution corresponding to the bremsstrahlung radiation spectrum is

$$\mathcal{G}_A(\mathbf{x}; k_t^2) \approx \frac{1}{k_t^2}; \quad (18)$$

In the saturation region, the gluon structure function is given by (3); the corresponding unintegrated gluon distribution has only logarithmic dependence on the transverse momentum:

$$\mathcal{G}_A(\mathbf{x}; k_t^2) \approx \frac{S_A}{s}; \quad k_t^2 < Q_s^2; \quad (19)$$

²At the time when this paper is being finalized, the result of the PHOBOS multiplicity measurement for central collisions has just been announced (see Note added).

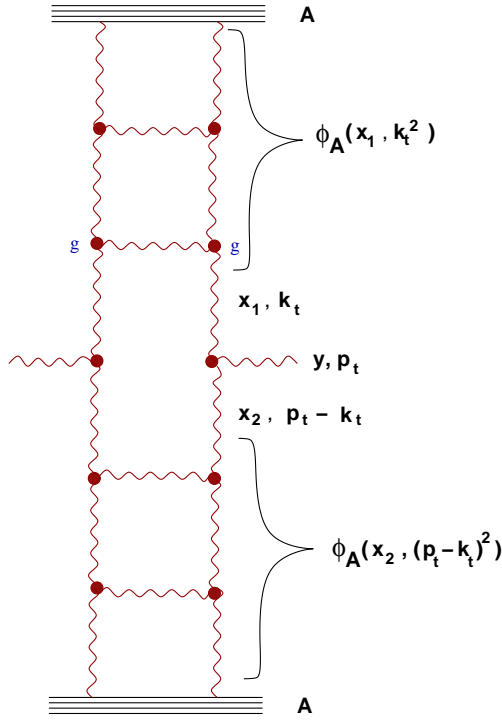


Figure 2: The Mueller diagram for the classical gluon radiation.

where S_A is the nuclear overlap area, determined by the atomic numbers of the colliding nuclei and by centrality of the collision.

The differential cross section of gluon production in a AA collision can now be written down as [L, 23]

$$E \frac{d}{d^3p} = \frac{4 N_c}{N_c^2} \frac{1}{1 p_t^2} \int dk_t^2 S_A(x_1; k_t^2) S_A(x_2; (p_t - k_t)^2); \quad (20)$$

where $x_{1,2} = (p_t = \bar{s}) \exp(\pm y)$, with y the (pseudo)rapidity of the produced gluon; the running coupling α_s has to be evaluated at the scale $Q^2 = \max(k_t^2; (p_t - k_t)^2)$. The rapidity density is then evaluated from (20) according to

$$\frac{dN}{dy} = \frac{1}{S_{AA}} \int d^2p_t E \frac{d}{d^3p}; \quad (21)$$

where S_{AA} is the inelastic cross section of nucleus-nucleus interaction.

Since the rapidity y and Bjorken variable x are related by $\ln(1-x) = y$, the x dependence of the gluon structure function translates into the following dependence of the saturation scale Q_s^2 on rapidity:

$$Q_s^2(s; y) = Q_s^2(s; y=0) \exp(\pm \lambda y); \quad (22)$$

As it follows from (22), the increase of rapidity at a fixed $W = \sqrt{s}$ moves the wave function of one of the colliding nuclei deeper into the saturation region, while leading to a smaller gluon density in the other, which as a result can be pushed out of the saturation domain. Therefore, depending on the value of rapidity, the integration over the transverse momentum in Eqs. (20), (21) can be split in two regions: i) the region $Q_{CD} < k_t < Q_{s,m}$ in which the wave

functions are both in the saturation domain; and ii) the region $Q_{s, \text{min}} < k_t < Q_{s, \text{max}}$ in which the wave function of one of the nuclei is in the saturation region and the other one is not. Of course, there is also the region of $k_t > Q_{s, \text{max}}$, which is governed by the usual perturbative dynamics, but our assumption here is that the rôle of these genuine hard processes in the bulk of gluon production is relatively small; in the saturation scenario, these processes represent quantum fluctuations above the classical background. It is worth commenting that in the conventional mini-jet picture, this classical background is absent, and the multi-particle production is dominated by perturbative processes. This is the main physical difference between the two approaches; for the production of particles with $p_t \gg Q_s$ they lead to identical results.

To perform the calculation according to (21), (20) away from $y = 0$ we need also to specify the behavior of the gluon structure function at large Bjorken x (and out of the saturation region). At $x \ll 1$, this behavior is governed by the QCD counting rules [24], $xG(x) \sim (1-x)^4$, so we adopt the following conventional form: $xG(x) \sim x(1-x)^4$.

We now have everything at hand to perform the integration over transverse momentum in (21), (20); the result is the following:

$$\frac{dN}{dy} = \text{const } S_A Q_{s, \text{min}}^2 \ln \frac{Q_{s, \text{min}}^2}{Q_{\text{CD}}^2} \left[1 + \frac{1}{2} \ln \frac{Q_{s, \text{max}}^2}{Q_{s, \text{min}}^2} \right] \left(\frac{Q_{s, \text{max}}}{s} \right)^3; \quad (23)$$

where the constant is energy-independent, S_A is the nuclear overlap area, $Q_s^2(s; y=0)$, and $Q_{s, \text{min}}^2$ ($Q_{s, \text{max}}^2$) are defined as the smaller (larger) values of (22); at $y = 0$, $Q_{s, \text{min}}^2 = Q_{s, \text{max}}^2 = Q_s^2(s) = Q_s^2(s_0) (s=s_0)^{-2}$. The first term in the brackets in (23) originates from the region in which both nuclear wave functions are in the saturation regime; this corresponds to the familiar

$(1-s) Q_s^2 R_A^2$ term in the gluon multiplicity, cf. Eq.(3). The second term comes from the region in which only one of the wave functions is in the saturation region.

The formula (20) has been derived using the form (19) for the unintegrated gluon distributions. We have checked numerically that the use of more sophisticated functional form of ρ_A taken from the saturation model of Golec-Biernat and Wustho [22] in Eq.(20) affects the results only at the level of about 3%.

Since $S_A Q_s^2 = N_{\text{part}} \frac{2}{Q_{\text{CD}}^2}$ (recall that $Q_s^2 = \frac{2}{Q_{\text{CD}}^2}$ is defined as the density of partons in the transverse plane, which is proportional to the density of participants), we can rewrite (23) in the following final form

$$\frac{dN}{dy} = c N_{\text{part}} \frac{s}{s_0} e^{-\eta} \ln \frac{Q_s^2}{Q_{\text{CD}}^2} \left[1 + \frac{1}{2} \ln \frac{Q_s}{s} \right] e^{-\eta/2} \left(\frac{Q_s}{s} \right)^3; \quad (24)$$

with $Q_s^2(s) = Q_s^2(s_0) (s=s_0)^{-2}$. This formula is the central result of our paper; it expresses the predictions of high density QCD for the energy, centrality, rapidity, and atomic number dependences of hadron multiplicities in nuclear collisions in terms of a single scaling function. Once the energy-independent constant $c = 1$ and $Q_s^2(s_0)$ are determined at some energy s_0 , Eq. (24) contains no free parameters. (The value of η , describing the growth of the gluon structure functions at small x can be determined in deep inelastic scattering; the HERA data are fitted

with $\beta = 0.25 - 0.3$ [22]). At $y = 0$ the expression (23) coincides exactly with the one derived in [7], and extends it to describe the rapidity and energy dependences.

Before we can compare (23) to the data, we have to take account of the difference between rapidity y and the measured pseudo-rapidity η . This is done by multiplying (23) by the Jacobian of the $y \leftrightarrow \eta$ transformation; a simple calculation yields

$$h(\eta; p_t; m) = \frac{\cosh y}{\frac{m^2 + p_t^2}{p_t^2} + \sinh^2 y}; \quad (25)$$

where m is the typical mass of the produced particle, and p_t is its typical transverse momentum. We thus have to make an assumption about the typical invariant mass of the gluon mini-jet. We estimate it by assuming that the slowest hadron in the mini-jet decay is the ρ -resonance; this leads to the invariant mass $m^2 = \sqrt{2} m_\rho Q_s$. Since the typical transverse momentum of the produced gluon mini-jet is Q_s , we take $p_t = Q_s$ in (25). The effect of the transformation from rapidity to pseudo-rapidity is the decrease of multiplicity at small η by about 10%, leading to the appearance of the dip in the pseudo-rapidity distribution in the vicinity of $\eta = 0$. We have checked that the change in the value of the mini-jet mass by two times affects the Jacobian at central pseudo-rapidity to about $\pm 10\%$, leading to $\pm 1\%$ effect on the final result.

The results for the Au-Au collisions at $\sqrt{s} = 130$ GeV are presented in Figs 3 and 4. In the calculation, we use the results on the dependence of saturation scale on the mean number of participants at $\sqrt{s} = 130$ GeV from [7], see Table 2 of that paper. The mean number of participants in a given centrality cut is taken from the PHOBOS paper [25]. One can see that both the centrality dependence and the rapidity dependence of the $\sqrt{s} = 130$ GeV PHOBOS data are well reproduced below $\eta = 4$. The rapidity dependence has been evaluated with $\beta = 0.25$, which is within the range $\beta = 0.25 - 0.3$ inferred from the HERA data [22]. The discrepancy above $\eta = 4$ is not surprising since our approach does not properly take into account multi-parton correlations which are important in the fragmentation region.

Our predictions for Au-Au collisions at $\sqrt{s} = 200$ GeV are presented in Figs. 5 and 6. The only parameter which governs the energy dependence is the exponent β , which we assume to be $\beta = 0.25$ as inferred from the HERA data. The absolute prediction for the multiplicity, as explained above, bears some uncertainty, but there is a definite feature of our scenario which is distinct from other approaches. It is the dependence of multiplicity on centrality, which around $\eta = 0$ is determined solely by the running of the QCD strong coupling [7]. As a result, the centrality dependence at $\sqrt{s} = 200$ GeV is somewhat less steep than at $\sqrt{s} = 130$. While the difference in the shape at these two energies is quite small, in the perturbative mini-jet picture this slope should increase, reflecting the growth of the mini-jet cross section with energy.

Let us confirm this statement quantitatively. The following simple parameterization [7] was found to describe the data [10, 11, 12] quite well:

$$\frac{dN}{d\eta} = (1 - X(s)) n_{pp} \frac{hN_{part}(\eta)}{2} + X(s) n_{pp} hN_{coll}(\eta); \quad (26)$$

where $hN_{part(coll)}$ are the average numbers of participants (collisions) for a given centrality, and $X(s)$ is an s -dependent parameter reflecting the relative strength of "soft" and "hard"

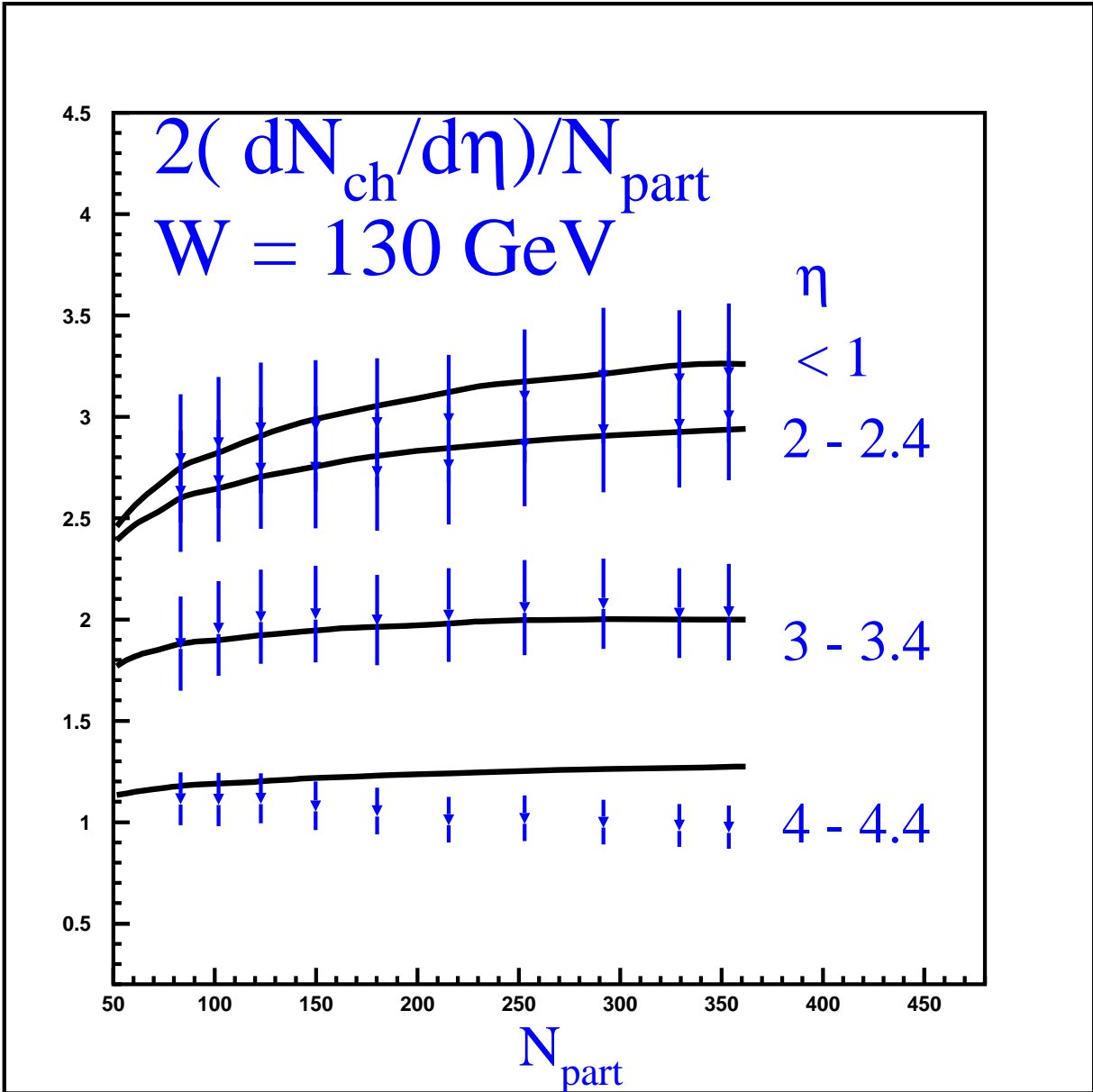


Figure 3: Centrality dependence of charged hadron production per participant at different pseudorapidity intervals in Au-Au collisions at $\sqrt{s} = 130 \text{ GeV}$; the data are from [25].

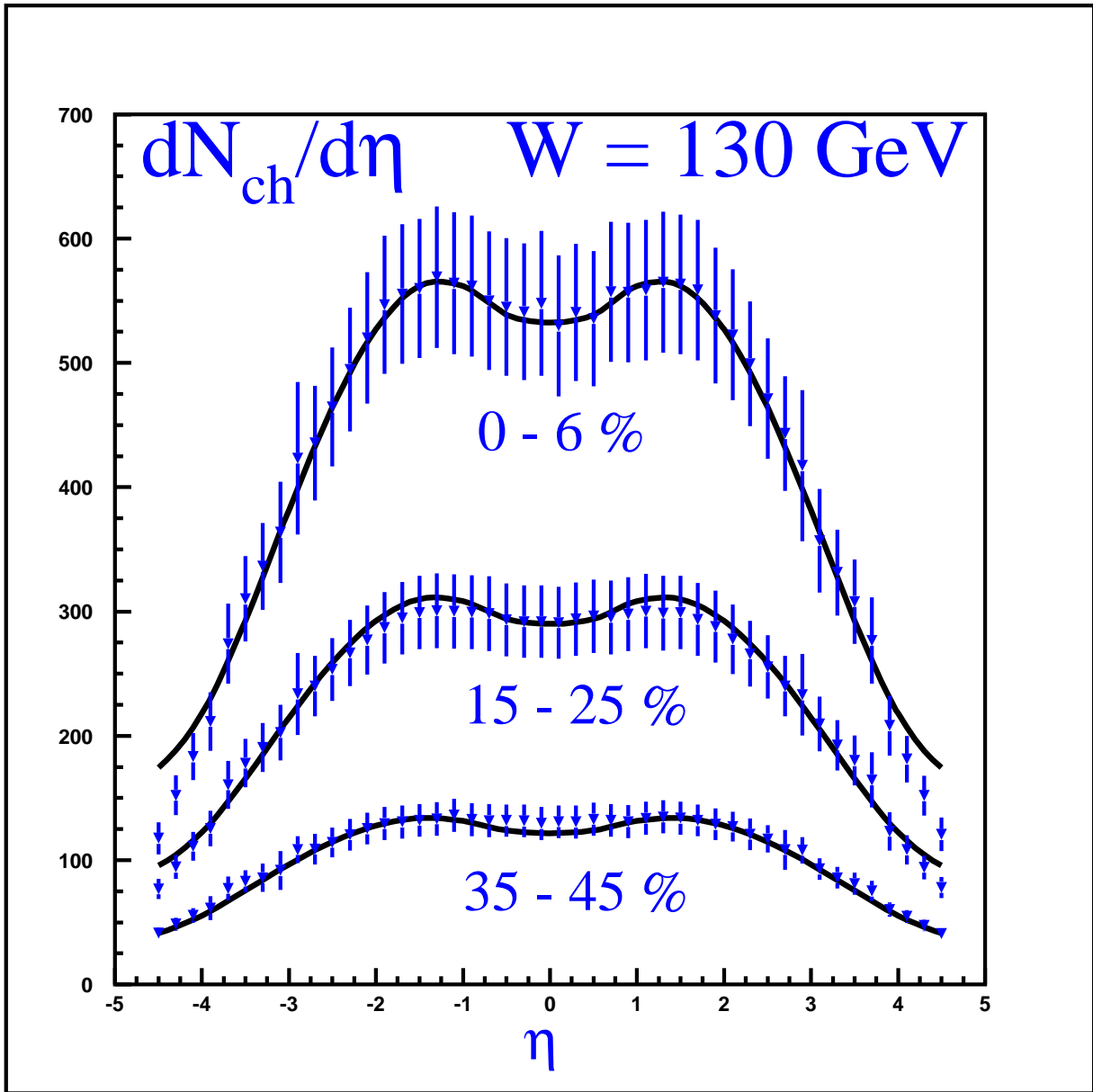


Figure 4: Pseudo-rapidity dependence of charged hadron production at different cuts on centrality in Au-Au collisions at $\sqrt{s} = 130 \text{ GeV}$; the data are from [25].

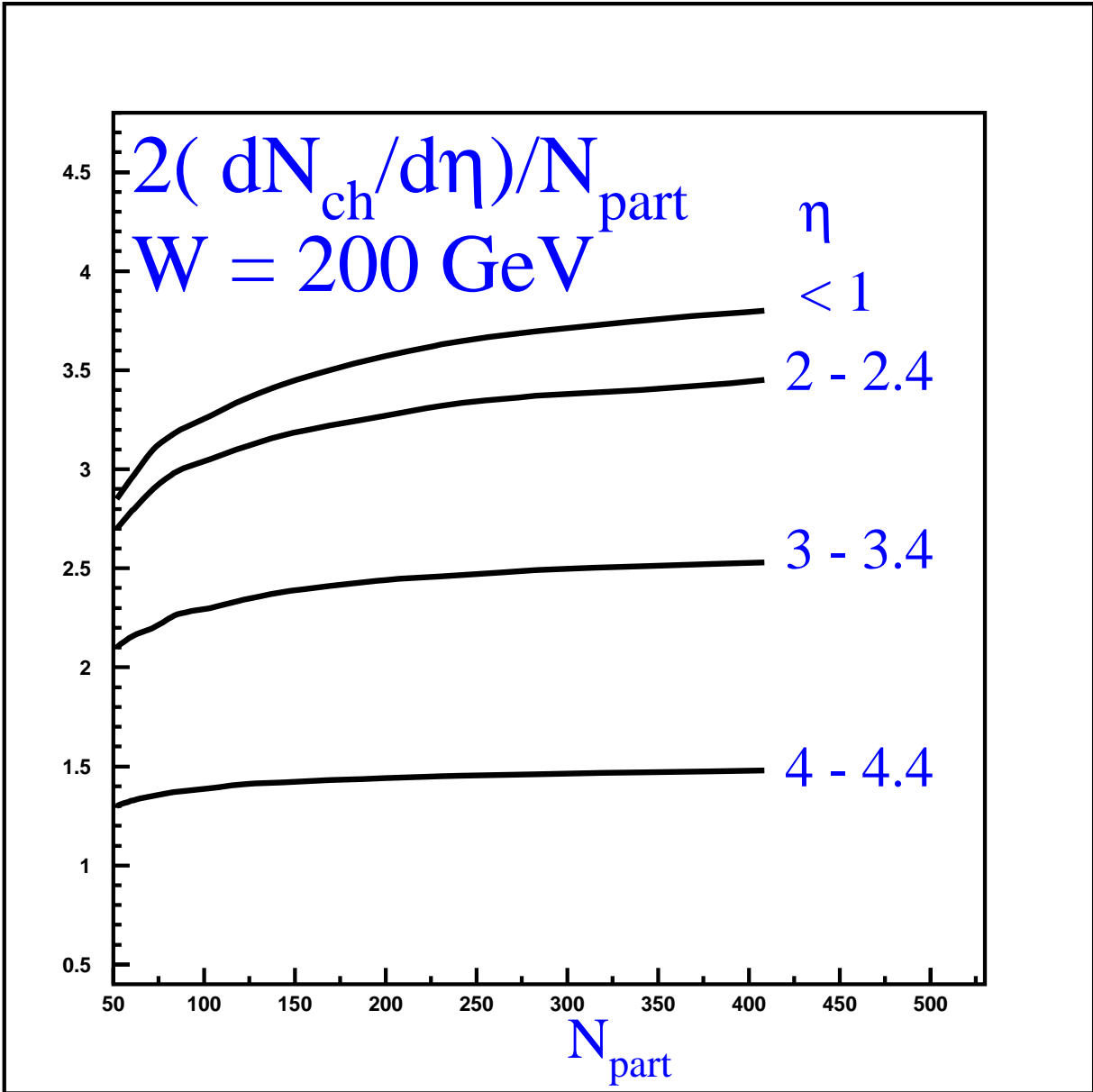


Figure 5: Centrality dependence of charged hadron production per participant at different pseudorapidity intervals in Au-Au collisions at $\sqrt{s} = 200 \text{ GeV}$.

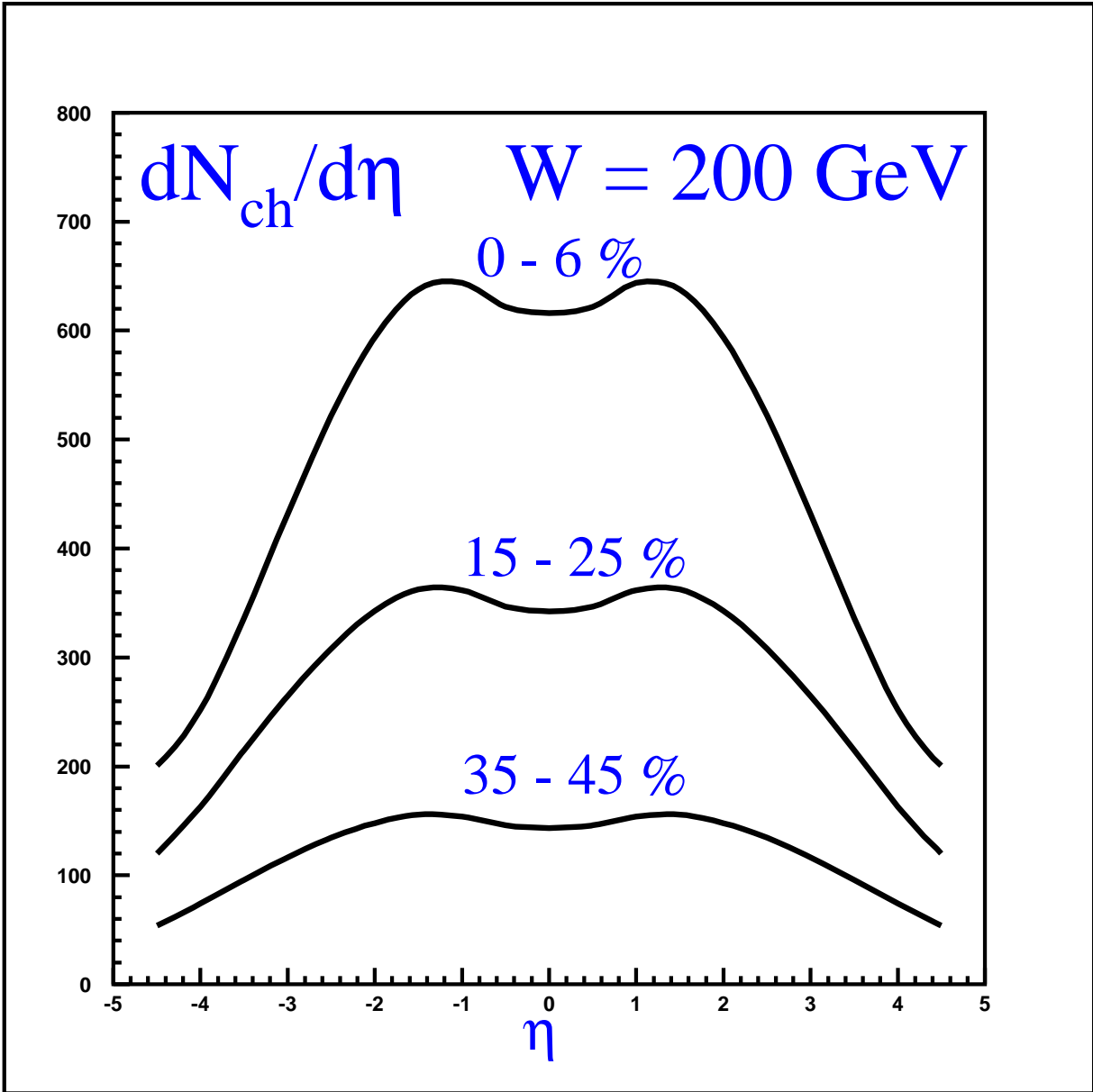


Figure 6: Pseudo-rapidity dependence of charged hadron production at different cuts on centrality in Au-Au collisions at $\sqrt{s} = 200$ GeV.

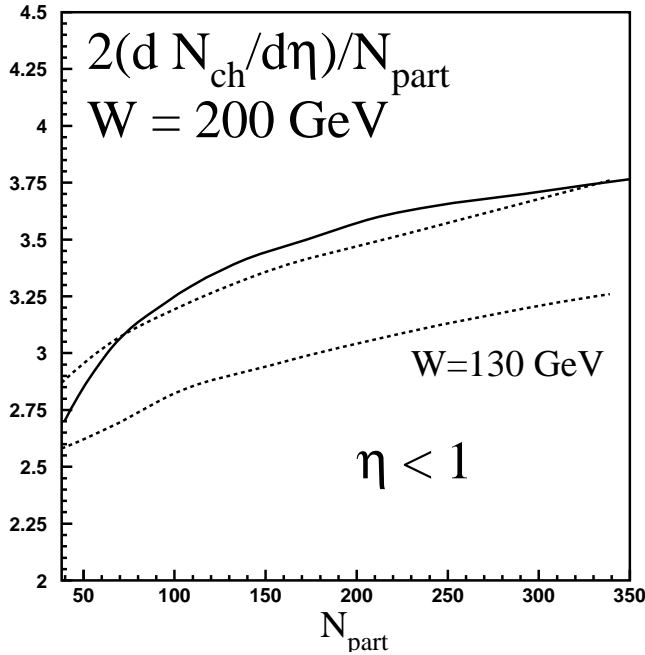


Figure 7: Comparison of the saturation (solid line) and "soft plus hard" (dashed line) calculations of the centrality dependence of charged hadron multiplicity at $\sqrt{s} = 200$ GeV; also shown is the "soft plus hard" calculation at $\sqrt{s} = 130$ GeV (lower dashed curve).

components in multiparticle production. At $\sqrt{s} = 130$ GeV, the value deduced from the central multiplicity was $X(130 \text{ GeV}) = 0.09 \pm 0.03$, and at $\sqrt{s} = 56$ GeV, it was $X(56 \text{ GeV}) = 0.05 \pm 0.03$. In the perturbative picture, the "hard" component of multiplicity is proportional to the mini-jet production cross section. At $\eta = 0$, the energy dependence of the mini-jet cross section is determined by the square of the gluon structure function $xG(x)$ (note that in the saturation approach, as we discussed above, it is the first power of $xG(x)$). Taking $xG(x) \propto x^{-\lambda}$, with $\lambda = 0.3$, translates then in the increase of the mini-jet production cross section by factor of $(130/56)^2 \approx 1.7$ in going from $\sqrt{s} = 56$ GeV to $\sqrt{s} = 130$ GeV, in accord with the ratio of the extracted values of $X(s)$ quoted above. Extrapolating the same energy dependence to $\sqrt{s} = 200$ GeV, we estimate

$$X(\sqrt{s} = 200 \text{ GeV}) = \frac{200^2}{130^2} X(\sqrt{s} = 130 \text{ GeV}) \approx 0.12 \pm 0.02; \quad (27)$$

where the error bar reflects only the uncertainty in the energy extrapolation of the central values of X . The value (27), together with Eq.(26), represents the prediction of the "soft plus hard" approach for the centrality dependence at $\sqrt{s} = 200$ GeV. Using the value (27) together with the average numbers of participants from [7] (see [26] for details of the Glauber model we use) $\langle N_{\text{part}} \rangle = 339$ and collisions $\langle N_{\text{coll}} \rangle = 1049$ in the 6% centrality cut at $\sqrt{s} = 200$ GeV, and the pp multiplicity of $n_{\text{pp}} = 2.43$ which follows from the parameterization of the data $n_{\text{pp}} = 2.5 - 0.25 \ln(s) + 0.023 \ln^2(s)$ [27, 25], we get the central value

$$\frac{dN}{d\eta}(\eta = 0) \approx 668; \quad (28)$$

which represents a $\sim 20\%$ increase compared to $\sqrt{s} = 130$ GeV. This value is larger than the one predicted above on the basis of the initial state saturation approach; however the main difference between the two scenarios will be in the centrality and rapidity dependences of hadron multiplicity.

To estimate the difference in the shape of centrality dependence, let us consider the case when the multiplicities in central collisions are forced to be the same and equal to $dN/d\eta = 634$, which is the upper limit of our prediction (16) and below the central value (28) (note that this represents the "worst case" in which the value of multiplicity in central collisions alone cannot be used to distinguish the two approaches). In the "soft plus hard" model, this multiplicity would then correspond to $X = 0.106$. In Fig. 7, we compare the resulting centrality dependences in the saturation and in the "soft plus hard" calculations. While the difference between the two curves is not large, the variation of the predictions with energy and rapidity could help to discriminate between the two approaches; for comparison, we also show the result of the "soft plus hard" calculation at $\sqrt{s} = 130$ GeV.

To summarize, we have extended the previous analysis [7] of multiparticle production in the quasi-classical picture to include the pseudo-rapidity dependence, and found good agreement with RHIC data at $\sqrt{s} = 130$ GeV. If this agreement persists at higher energies, one may conclude that the dynamics of quasi-classical color fields, encoded in our approach in terms of a simple scaling function (24), describes well the gross features of multiparticle production already at RHIC energy. The experimental study of centrality and rapidity dependences at $\sqrt{s} = 200$ GeV will thus be a very important step in establishing the presence of high density QCD effects in relativistic nuclear collisions. The clear discrimination between this and other approaches may however require the study of more "microscopic" observables.

Note added: While we were finalizing this paper, the first $\sqrt{s} = 200$ GeV multiplicity measurement by the PHOBOS Collaboration had been announced [28]. The ratio of multiplicities in the central (0–6% centrality cut) events at $\sqrt{s} = 200$ and $\sqrt{s} = 130$ GeV has been reported: $R(200=130) = 1.14 \pm 0.06$. While this is in accord with the prediction based on the saturation approach given above, $R(200=130) = 1.10 \pm 1.14$, it is also consistent with the 20% increase which we expect in the "soft plus hard" scenario. (We did not attempt to adjust to the central value of the announced data our calculations shown in Figs 5 and 6 and reported (e.g., [29]) before the multiplicity in head-on collisions had been available). The crucial test of the quasi-classical approach will thus be provided by the centrality and pseudo-rapidity dependences of hadron multiplicities.

The work of D.K. was supported by the US Department of Energy (Contract # DE-AC02-98CH10886). The research of E.L. was supported in part by the Israel Science Foundation, founded by the Israeli Academy of Science and Humanities, and BSF # 9800276.

References

- [1] L.V.Gribov, E.M.Levin and M.G.Ryskin, *Phys.Rep.* 100 (1983) 1.
- [2] A.H.Mueller and J.Qiu, *Nucl.Phys.B* 268 (1986) 427.
- [3] J.P.Blaizot and A.H.Mueller, *Nucl.Phys.B* 289 (1987) 847.
- [4] L.McLerran and R.Venugopalan, *Phys.Rev.D* 49 (1994) 2233, 3352; *D* 50 (1994) 2225, *D* 53 (1996) 458, *D* 59 (1999) 094002.
- [5] E.Tancu and L.McLerran, *Phys.Lett.B* 510 (2001) 145; Yu.Kovchegov, *Phys.Rev.D* 54 (1996) 5463; [hep-ph/0011252](#); A.Krasnitz and R.Venugopalan, *Phys.Rev.Lett.* 84 (2000) 4309; E.Levin and K.Tuchin, *Nucl.Phys.B* 573 (2000) 833.
- [6] Ia.Balitsky, *Nucl.Phys.B* 463 (1996) 99; Yu.Kovchegov, *Phys.Rev.D* 60 (2000) 034008.
- [7] D.Kharzeev and M.Nardi, *Phys.Lett.B* 507 (2001) 121.
- [8] D.Kharzeev and E.Levin, *Nucl.Phys.B* 578 (2000) 351; D.Kharzeev, Yu.Kovchegov and E.Levin, *Nucl.Phys.A* 690 (2001) 621; [hep-ph/0106248](#).
- [9] E.V.Shuryak, *Phys.Lett.B* 486 (2000) 378; [hep-ph/0101269](#); M.Nowak, E.Shuryak and I.Zahed, *Phys.Rev.D* 64 (2001) 034008.
- [10] B.Back et al, PHOBOS Coll, *Phys.Rev.Lett.* 85 (2000) 3100; [nucl-ex/0105011](#); [nucl-ex/0106006](#).
- [11] K.Adox et al, PHENIX Coll, *Phys.Rev.Lett.* 86 (2001) 3500; [nucl-ex/0012008](#); [nucl-ex/0104015](#).
- [12] C.Adler et al, STAR Coll, [nucl-ex/0106004](#).
- [13] F.Videbaek et al, BRAHMS Coll, <http://www.rhic.bnl.gov/qm> 2001.
- [14] X.N.Wang and M.Gyulassy, *Phys.Rev.Lett.* 86 (2001) 3496.
- [15] K.J.Eskola, K.Kajantie, P.V.Ruuskanen, K.Tuominen, *Nucl.Phys.B* 570 (2000) 379; K.J.Eskola, K.Kajantie, K.Tuominen, *Phys.Lett.B* 497 (2001) 39; [hep-ph/0106330](#).
- [16] A.Capella and D.Sousa, *Phys.Lett.B* 511 (2001) 185.
- [17] S.Jeon and J.Kapusta, *Phys.Rev.C* 63 (2001) 011901; N.Amesto, C.Pajares, D.Sousa, [hep-ph/0104269](#); D.E.Kahana and S.H.Kahana, *Phys.Rev.C* 63 (2001) 031901; A.Accardi, [hep-ph/0107301](#).
- [18] D.Kharzeev, [nucl-th/0107033](#).

- [19] A. H. Mueller, Nucl. Phys. B 572 (2000) 227.
- [20] A. Krasnitz and R. Venugopalan, Phys. Rev. Lett. 86 (2001) 1717.
- [21] Yu. Kovchegov, hep-ph/0011252.
- [22] K. Golec-Biernat and M. Wusthof, Phys. Rev. D 59 (1999) 014017; Phys. Rev. D 60 (1999) 114023; A. Stasto, K. Golec-Biernat and J. Kwiecinski, Phys. Rev. Lett. 86 (2001) 596.
- [23] M. Gyulassy and L. McLerran, Phys. Rev. C 56 (1997) 2219.
- [24] G. Farrar and S.J. Brodsky, Phys. Rev. Lett. 31 (1973) 1153;
V.A. Matveev, R.M. Muradian, A.N. Tavkhelidze, Lett. Nuovo Cim. 7 (1973) 719.
- [25] B. Back et al., PHOBOS Coll., nucl-ex/0106006.
- [26] D. Kharzeev, C. Lourenco, M. Nardi and H. Satz, Z. Phys. C 74 (1997) 307.
- [27] F. Abe et al., CDF Coll., Phys. Rev. D 41 (1990) 2330.
- [28] B. Wysluch, PHOBOS Coll., Talk at the INPC 2001, Berkeley, USA, July 30 - August 2, 2001.
- [29] D. Kharzeev, Talk at the "Glauber approach at RHIC" Workshop, BNL, July 19, 2001;
<http://www.phobos.bnl.gov/GlauberWorkshop.htm>